

CrystEngComm

Accepted Manuscript



This is an *Accepted Manuscript*, which has been through the Royal Society of Chemistry peer review process and has been accepted for publication.

Accepted Manuscripts are published online shortly after acceptance, before technical editing, formatting and proof reading. Using this free service, authors can make their results available to the community, in citable form, before we publish the edited article. We will replace this *Accepted Manuscript* with the edited and formatted *Advance Article* as soon as it is available.

You can find more information about *Accepted Manuscripts* in the [Information for Authors](#).

Please note that technical editing may introduce minor changes to the text and/or graphics, which may alter content. The journal's standard [Terms & Conditions](#) and the [Ethical guidelines](#) still apply. In no event shall the Royal Society of Chemistry be held responsible for any errors or omissions in this *Accepted Manuscript* or any consequences arising from the use of any information it contains.

Cite this: DOI: 10.1039/c0xx00000x

www.rsc.org/xxxxxx

ARTICLE TYPE

Yolk-shell ZnWO₄ microspheres: One-pot synthesis, characterization and photocatalytic properties

Miao Wang*, Yanfeng Tang, Tongming Sun, Guoqing Jiang* and Yujun Shi

Received (in XXX, XXX) Xth XXXXXXXXX 20XX, Accepted Xth XXXXXXXXX 20XX

DOI: 10.1039/b000000x

Abstract: Novel yolk-shell ZnWO₄ microspheres have been fabricated via a one-pot hydrothermal process in the presence of L-Aspartic acid (L-Asp). The as-obtained products are characterized by X-ray diffraction, scanning electron microscopy, transmission electron microscopy, nitrogen adsorption-desorption experimentation and UV-vis absorption spectroscopy, respectively. The effects of reaction conditions on the morphology and crystallinity of products are studied, as well as the amounts of L-Asp, reaction time and reaction temperature. As the chelating agent and shape modifier, L-Asp plays a key role in crystal growth of yolk-shell ZnWO₄ microspheres. A possible formation mechanism for the yolk-shell microspheres is proposed. The photocatalytic properties of the yolk-shell ZnWO₄ microspheres are investigated by the decomposition of Rhodamine B (RhB) and methylene blue (MB) under UV light irradiation and the results show that they have excellent photocatalytic activities. Furthermore, the obtained yolk-shell ZnWO₄ microspheres are chemically stable and the efficiency remained almost the same after recycled five times, suggesting that the yolk-shell ZnWO₄ microspheres are promising photocatalysts for practical applications.

Introduction

Recently, as a new special class of core-shell nanostructures, yolk-shell structures with interior core, void space, and permeable outer shell have received increasing attention because of their unique properties (such as low density, large surface area, high permeability, and excellent loading capacity) and their great potential for application in drug delivery, lithium-ion batteries, sensing, and catalysis.¹⁻⁷ Thus far, a variety of strategies have been explored for the synthesis of yolk-shell structures, which involve template-assisted,⁸⁻¹² Kirkendall effect,¹³⁻¹⁴ galvanic reaction,¹⁵⁻¹⁷ and Ostwald ripening based methods.¹⁸⁻¹⁹ However, these methods are limited by their complexity and the choice of appropriate surfactant or template systems. Meanwhile, most of these methods need the pre-preparation of core particles, following multistep and complex chemical procedures. Therefore, from the point of view of economical and environmentally friendly, development of mild, low-cost, one-pot and template-free strategies for controlling synthesis yolk-shell micro/nanostructures will be more attractive and highly desirable for the practical application.

ZnWO₄, as one of the important metal tungstates, has attracted wide interest due to its widespread and potential applications in various fields, such as scintillators, solid-state laser hosts, photocatalysts, gas and humidity sensors, optical fibers and electronic materials.²⁰⁻²⁹ For the sake of further enhancing the properties and extending the applications of materials, their preparation with novel structures has attracted significant attention. As well known, the intrinsic properties of nanoscale materials are mainly determined by their crystallinity, dimension and morphology. In the past decade, various morphological ZnWO₄ nano/microstructures (rods, wires, hollow microspheres, hollow clusters and chrysanthemum-shape) have been synthesized through solid-state, precipitation, sol-gel,

hydro/solvothermal and microwave routes.²⁵⁻³⁷ However, works focused on the preparation of yolk-shell ZnWO₄ particles are relatively rare.

Biomolecule-assisted route has been proved to be a novel, eco-friendly, and promising method for the formation of various materials. Amino acid or other biological molecules usually serve as structure directing agents to alter the morphology of micro/nanostructures by preferentially interacting with certain crystal faces and modifying the overall crystal shape. In this paper, we report the successful preparation of yolk-shell ZnWO₄ microspheres via L-Asp assisted hydrothermal route. This mild and one-pot method does not need any hard or soft template, avoiding the procedures and cost for their removal in the product. Meanwhile, the importance of reaction time, temperature and L-Asp were discussed in detail. In addition, the possible formation mechanism of yolk-shell ZnWO₄ microspheres was also demonstrated. Furthermore, the photocatalytic activities of the yolk-shell ZnWO₄ microspheres were investigated by the decomposition of RhB under UV light irradiation.

Experimental Section

All the chemicals including L-Asp, Na₂WO₄·2H₂O and ZnSO₄·7H₂O are analytical grade and used without further purification. A typical procedure for the preparation of yolk-shell ZnWO₄ microspheres is given below. 1.0 mmol ZnSO₄·7H₂O and 1.0 mmol L-Asp were dissolved in 25 mL distilled water and the mixture was stirred for 20 min, then 1.0 mmol Na₂WO₄·2H₂O was added. Stirring for 30 min, the obtained suspension was transferred into a 30 mL Teflon-lined autoclave. After being sealed and heated at 150 °C for 12 h, the

autoclave was gradually cooled to room temperature. The products was precipitated by centrifugation, washed with distilled water and ethanol and finally dried at 70 °C for 3 h.

The photocatalytic activity of the as-prepared yolk-shell ZnWO₄ microspheres was evaluated by photocatalytic decolorization of RhB and MB aqueous solution under UV light irradiation. A 250 W high-pressure mercury lamp was used as a light source and an electric fan and cycled condensate water were used to prevent thermal catalytic effects. In a typical experiment, the as-prepared 30 mg yolk-shell ZnWO₄ microspheres was added into 50 mL of the RhB or MB (20 mg L⁻¹) solution. Before light was turned on, the solution was continuously stirred for 30 min in the dark to ensure the establishment of an adsorption-desorption equilibrium. During irradiation, 3.5 mL of the suspension was continually taken from the reactor at given time intervals. The photocatalyst powders and the pollutions solution were separated by a centrifugal machine. The process was monitored by using a UV-vis spectrometer. For comparison, the commercial Degussa P25 was also examined under the same conditions.

X-ray diffraction (XRD) patterns were recorded on a Bruker AXSD8 ADVANCE X-ray diffractometer (Cu K α radiation λ = 0.15418 nm) at room temperature. The operation voltage and current were maintained at 40 kV and 40 mA, respectively. The morphologies and microstructures of the as-synthesized samples were studied by scanning electron microscopy (SEM, Hitachi S-4800) employing an operating voltage of 15 kV and transmission electron microscopy (TEM, JEOL-2100F) under 200 kV accelerating voltage. Nitrogen adsorption-desorption analysis was performed with a Micromeritics ASAP 2020C apparatus. The UV-vis spectrum of the sample was analyzed with a UV-vis spectrophotometer (UV-3600, Shimadzu, Japan). The concentration of RhB solution was analyzed through Shimadzu UV-2401PC spectrophotometer.

Results and discussion

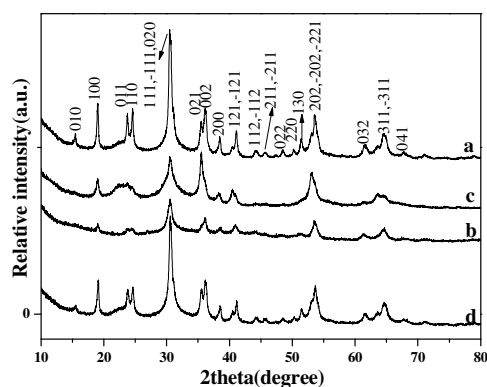


Fig. 1 XRD patterns of the products obtained from different time: (a)12h; (b) 1h; (c) 3h; (d) 6h

The phase purity of the samples are examined by XRD. Fig. 1 show the XRD patterns of the as-prepared samples for the time-dependent experiments. As shown in Fig. 1a, all peaks of the sample prepared in the typical procedure can be indexed to tetragonal phase of ZnWO₄ (JCPDS card No. 15-0744). The

strong and sharp peaks suggest that the products are well-crystalline. For comparison, other similar experiments were carried out by modulating the reaction time. As shown in Fig.1b-d, all samples are all pure tetragonal phase of ZnWO₄. The results indicate that reaction time has no obvious effect on the phase of the products. However, the diffraction peaks of the samples obtained within 12 h are much sharper than those of obtained from 1 h and 3 h, revealing the improved crystalline after prolonging the reaction time.

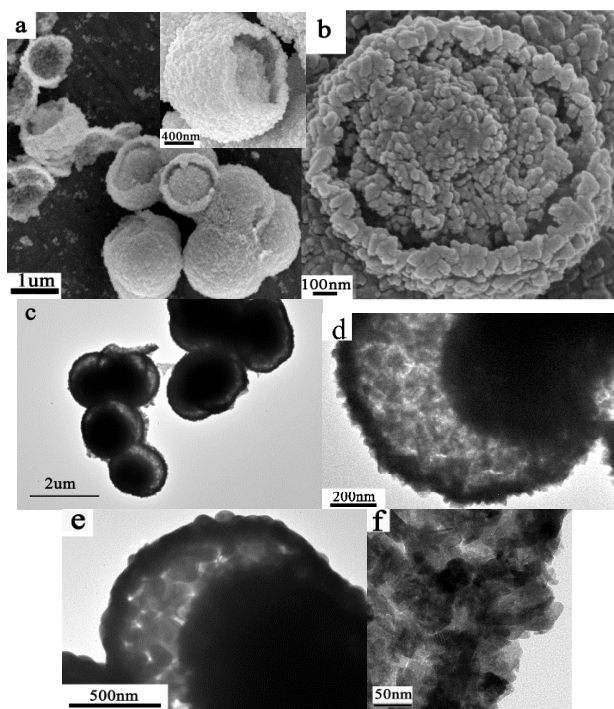


Fig. 2 SEM (a-b) and TEM (c-f) images of the product obtained in a typical procedure.

The dimensions and morphologies of the products are characterized by SEM and TEM. Fig. 2 shows the SEM and TEM images of the ZnWO₄ prepared in the typical procedure. The low-magnified SEM image (Fig. 2a) shows that there are many aggregated yolk-shell microspheres, and some cores and shells are divided. From the images, the outer diameter of the spheres is about 1.5 μ m, while the inner hollow core diameter is about 1 μ m. The close-up view (inset Fig. 2a) further demonstrates that the core and the shell are separated and there is a large void space between them. The SEM image (Fig. 2b) from a single yolk-shell microsphere indicates that the core and the shell are consist of a large number of small nanoparticles with the size of 50-100 nm, suggesting that they are derived from nanoparticles aggregation. The microstructures of the sample are further characterized by TEM. The TEM images (Fig. 2c-d) reveal that the core and the shell are separated, and there is a strong contrast difference between the core (dark) and shell (bright). Furthermore, the coarse shell of the yolk-shell ZnWO₄ spheres is actually made of fine nanoparticles with the size of about 50-100 nm and the shell thickness is about 150 nm (Fig. 2e-f), which is consistent with the corresponding SEM

images. This interesting yolk-shell structure is similar with the reported TiO_2 spheres, named as sphere-in-sphere structure.³⁸

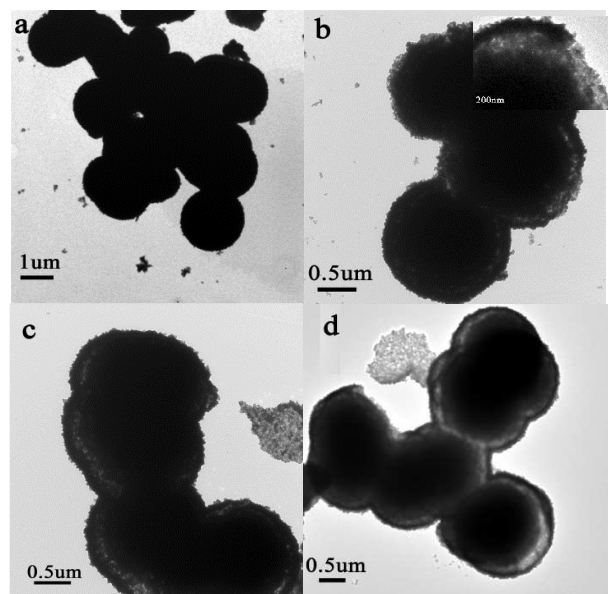


Fig. 3 TEM images of the products obtained from different reaction time: (a) 1 h; (b) 3 h; (c) 6 h; (d) 9 h

A series of time-dependent experiments are carried out to investigate the formation process and the growth mechanism of yolk-shell ZnWO_4 microspheres by analyzing the samples collected at different growth periods. The TEM images of morphological evolution of the products obtained after the reaction for different times are shown in Fig. 3. Fig. 3a displays that the samples obtained from 1 h, there are a large amount of aggregated solid microspheres with diameter of 1-1.5 μm and the surface is not smooth. After 3 h of reaction, as shown in Fig. 3b, there are light rings in some microspheres when the electron is penetrate. The magnified shell edge of the a single sphere (inset Fig. 3b) confirms that the sphere is formed by aggregation of nanoparticles with a size of 50 nm. The original solid sphere is separated into two discrete parts of core and shell. Further prolonging time to 6 h and 9 h, the yolk-shell structures are observed obviously (Fig. 3c-d). With the diameter of the core is decreased, the void space between core and shell is becoming larger and larger. Yolk-shell microspheres with much thinner shell gradually emerged. Therefore, with the increase of the reaction time, the as obtained ZnWO_4 undergo a morphological evolution from nanoparticles-aggregated solid spheres to yolk-shell microspheres.

The influence of temperature on the crystalline phase and morphology of the product are also investigated. Fig. 4a shows the XRD patterns of the products obtained from different temperature. The diffraction peaks of the products prepared at 150 $^\circ\text{C}$ are much sharper than those of 120 $^\circ\text{C}$ and 100 $^\circ\text{C}$. There is no obvious peak when the reaction was conducted at 100 $^\circ\text{C}$ for 12 h, indicating the sample are amorphous status. Therefore, the crystalline of the products are improved with the increasing of reaction temperature. Herein, to meet the requirements of homogeneous nucleation, the reaction was carried out at a higher temperature (150 $^\circ\text{C}$). When 1 mmol L-Asp is used, the SEM

images of the products obtained from different hydrothermal temperature are shown in Fig. 4b-c. When the reaction is carried out at 100 $^\circ\text{C}$, there are many aggregated nanoparticles (Fig. 4b). As shown in Fig. 4c, when the reaction temperature are increased from 100 $^\circ\text{C}$ to 120 $^\circ\text{C}$, the morphologies of the products are varied from nanoparticles to nanoparticles-assembled microspheres. As mentioned above, no yolk-shell microspheres are observed, indicating that reaction temperature plays an important role in the formation of yolk-shell ZnWO_4 microspheres. A higher temperature is necessary for the nucleation and crystal growth process of nanostructures.

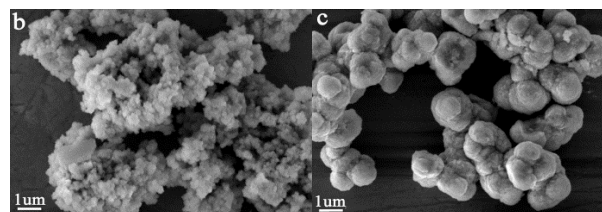
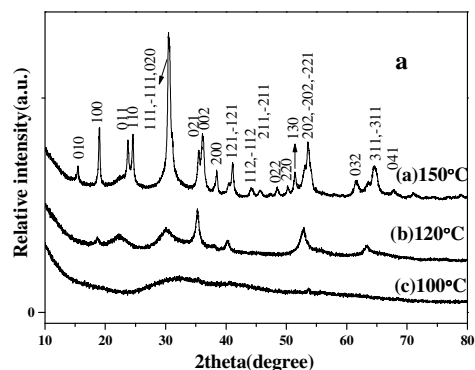


Fig. 4 XRD patterns (a) and SEM images of the products obtained from different temperature: (b) 100 $^\circ\text{C}$; (c) 120 $^\circ\text{C}$.

To obtain a better understanding of the formation process of yolk-shell microspheres, controlled trials are performed to investigate the effect of L-Asp on the morphologies of the products. When all the parameters except L-Asp are kept identical, the corresponding SEM and TEM images of products obtained from 12 h are shown in Fig. 5. In the absence of L-Asp, a large number of nanorods are formed with diameter of 50 nm (Fig. 5a-b). In case of 1 mmol L-Asp is used, there are many uniform yolk-shell microspheres formed (Fig. 5c-d). As the amount of L-Asp is increased to 2 mmol (Fig. 5e-f), the morphology of the as-obtained ZnWO_4 are aggregated microspheres with diameter about 3-5 μm . These observations indicate that L-Asp is a key factor in controlling the morphologies of the products. The L-Asp molecular are used as structure directing agents in the reaction system. Consequently, the morphologies of the as-prepared ZnWO_4 are dependent on the amount of the L-Asp.

Aspartic acid (Asp) is an amino acid with the chemical formula $\text{HOOCCH}(\text{NH}_2)\text{CH}_2\text{COOH}$. In our previous work, it is found that the L-Asp assisted method may provide an alternative for controlling of inorganic crystal growth and fabricating novel micro/nanostructures, such as nanobelts-assembled flower-like $\text{Zn}_3(\text{OH})_2\text{V}_2\text{O}_7 \cdot 2\text{H}_2\text{O}$ microcrystals³⁹ and hierarchical

nanowires-assembled YVO_4 microspheres.⁴⁰ Therefore, as a toxic-free, economical, and eco-friendly biomolecule, L-Asp assisted method may provide an eco-friendly opportunity to synthesize other inorganic micro/nanomaterials with uniform size and controllable morphology.

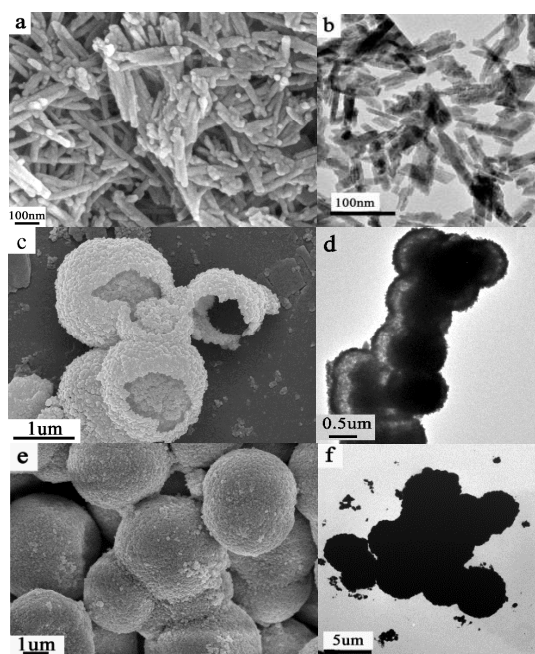


Fig. 5 SEM and TEM images of the products obtained from different amount of L-Asp within 12 h. (a-b) 0 mmol; (c-d) 1 mmol; (e-f) 2 mmol.

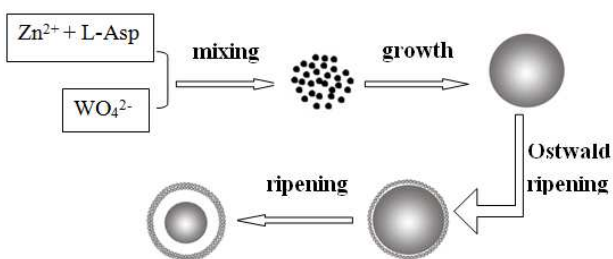


Fig. 6 Schematic illustration of the formation mechanism of yolk-shell ZnWO_4 microspheres.

From the above experimental results, a possible formation mechanism is proposed. A concise schematic illustration for the process of the shape evolution is shown in Fig. 6. Ostwald ripening is a feasible mechanism for the formation of the yolk-shell ZnWO_4 microspheres. As well known, the groups $-\text{NH}_2$ and $-\text{COOH}$ in L-Asp can all be coordinated with Zn^{2+} . In the first step, Zn^{2+} and L-Asp form complexes at the beginning. The WO_4^{2-} reacts with the Zn^{2+} ions (released from the Zn-Asp complex) to form ZnWO_4 nanoparticles. Thus, ZnWO_4 nanoparticles are formed from the reaction Zn^{2+} , L-Asp and WO_4^{2-} at the initial stage of reaction. In the second step, the tiny ZnWO_4 nanoparticles are aggregate together and grow into nanoparticles-assembled solid spheres in the presence of proper amount of L-Asp, as shown in Fig. 3a. In the third step, with

the increasing of reaction time, a void which is surrounded by the re-crystallized shell is created as the inner particles are dissolved. As a result, the void space divides the solid sphere into two separate regions to shape a core-shell structure. During the ripening process, the core-shell microspheres are slow dissolved from the inner, which promotes the transportation of nanoparticles from inner core to outer surface (Fig. 3b-d). In the fourth step, the cores in the center of the microspheres could be gradually consumed mainly through the Ostwald ripening process (crystallites grow at the expense of the smaller ones), resulting in the formation of yolk-shell ZnWO_4 microspheres.

This phenomenon has also been found in the synthesis of hollow spheres⁴¹⁻⁴⁴ and other yolk-shell particles.¹⁸⁻¹⁹

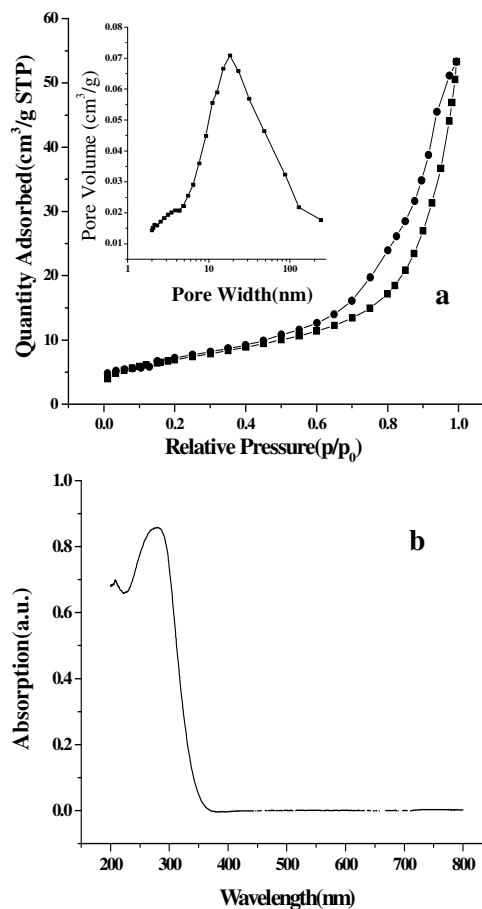


Fig. 7 (a) N_2 adsorption-desorption isotherm and BJH desorption pore width distribution (inset) of yolk-shell ZnWO_4 microspheres. (b) UV-vis spectrum of the yolk-shell ZnWO_4 microspheres.

The surface area and pore size distribution of yolk-shell ZnWO_4 spheres are determined by nitrogen adsorption-desorption isotherm, as shown in Fig. 7a. The isotherm of the yolk-shell microspheres is characteristic of the type II isotherm. The adsorption and desorption isotherm depicts a pregnant hysteresis loop in the relative pressure range of 0.4-1.0, which reveals that the ZnWO_4 is a mesoporous material.⁴⁵⁻⁴⁶ The presence of hysteresis reveals the existence of hollow structures in the sample, which is in agreement with SEM and TEM observations (Fig. 2). The Brunauer-Emmett-Teller (BET) surface of the yolk-shell ZnWO_4 microspheres is $24.5984 \text{ m}^2/\text{g}$. The pore size

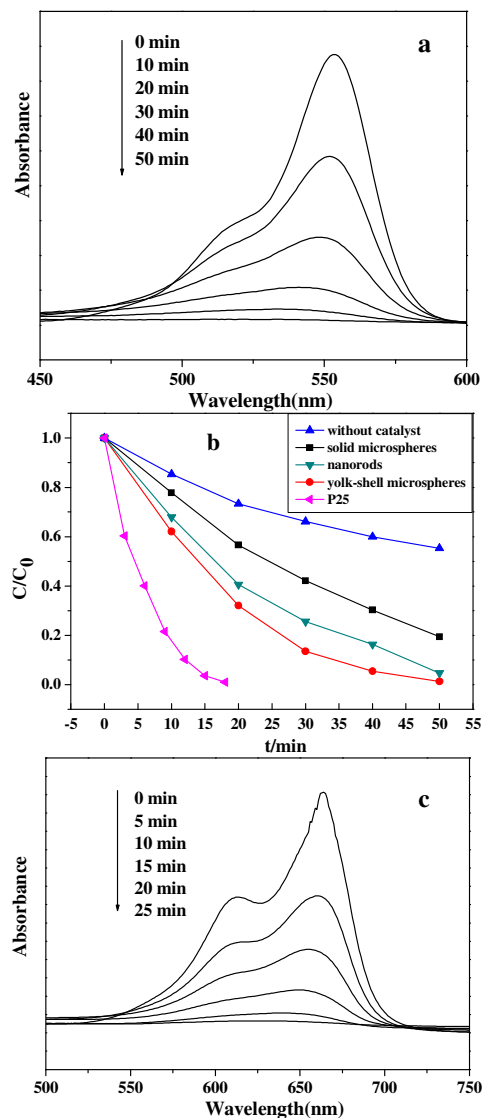
distribution is calculated from the desorption branch of the nitrogen isotherm by the Barrett-Joyner-Halenda (BJH) method, as shown in Fig. 7a inset. The results show that the average pore width of resultant yolk-shell ZnWO_4 spheres is approximately 17.97 nm, and the pore volume is $0.08313 \text{ cm}^3/\text{g}$.

As well known, the optical absorption property of the materials is considered as a pivotal factor in determining its photocatalytic activity. Therefore, before the photocatalytic activity characterization, it is important to study the optical absorption of the as-prepared ZnWO_4 . Fig. 7b shows the UV-Vis spectrum of yolk-shell ZnWO_4 microspheres. The yolk-shell ZnWO_4 microspheres present intense absorption from 220-370 nm. Therefore, the catalyst has absorption in the UV region. The color of ZnWO_4 powder is white, as can be expected from the absorption spectrum.

To test the potential applicability of the as-synthesized ZnWO_4 as a photocatalyst, the photodegradation of RhB is chosen as a facile model process to investigate their photocatalytic activity under UV light irradiation. The characteristic absorption of RhB at 552 nm is used to monitor the degradation process as a function of irradiation time. The suspension is stirred in the dark for 30 min to achieve the adsorption-desorption equilibrium before being irradiated with UV light. It is found that the intensity of the characteristic adsorption peak decreased with the increase of irradiation time in the degradation process and almost disappeared after 50 min (Fig. 8a). The change of the absorption spectra of RhB aqueous solution represents the change in the concentration. This decrease in absorption is accompanied with a slight shift of the main absorption peak to lower wavelength due to the formation of the demethylated dyes. Fig. 8b shows the photodegradation efficiency of RhB as a function of irradiation time with different morphological ZnWO_4 photocatalysts. C is the absorption of RhB at time t and C_0 is the absorption of RhB before irradiation. The yolk-shell ZnWO_4 microspheres exhibit excellent photocatalytic activities for degradation of RhB under UV light irradiation. Contrarily, the degradation of RhB was very slow without photocatalysts. It can be seen that the adsorption ability of yolk-shell ZnWO_4 microspheres is much higher than the ZnWO_4 solid microspheres (obtained from 1 h) because of its hollow structure and larger BET surface areas. Meanwhile, in spite of showing relatively low BET surface area, the adsorption ability of yolk-shell ZnWO_4 microspheres is slightly higher than the ZnWO_4 nanorods (obtained without L-Asp) because of its porous hollow structure.

MB is a very stable dye and has been used in photocatalytic decoloration. In order to further confirm the photocatalytic activities of these samples under UV light irradiation, the photocatalytic decoloration of MB solution by these samples was also investigated under the same conditions. Fig. 8c shows the temporal evolution of the absorption spectra during the photocatalytic degradation of MB in the presence of the yolk-shell ZnWO_4 microspheres. The MB solution shows an intense absorption band centered at 664 nm. Compared with RhB, MB solution is much easier to be decolorized. MB is degraded in 25 min in the presence of the yolk-shell ZnWO_4 microspheres. Similarly, the yolk-shell ZnWO_4 microspheres show the highest activity among all samples, as shown in Fig. 8d. The

improvement of the photocatalytic activities of the yolk-shell ZnWO_4 might be benefit from the multiple reflection of the light due to the special yolk-shell structure.⁴⁷⁻⁴⁸ This indicates that the photocatalytic activity of the catalyst is the syngesitic result of many factors, such as size, crystallinity, morphology and BET surface areas. The porous surface and its interior hollow cavity of yolk-shell structure allows multiple reflections of UV light are critical for catalyst, and increases the quantity of photogenerated electrons and holes available to participate in the photocatalytic decomposition of RhB, thus offering an improved catalytic activity. The above results suggest that such unique yolk-shell structure provides ZnWO_4 with excellent photocatalytic activity.



75

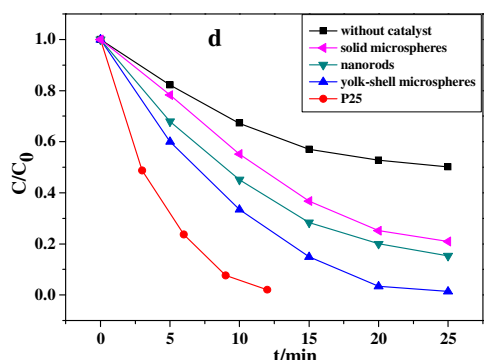


Fig. 8 Absorption spectra of the RhB (a) and MB (c) in the presence of yolk-shell ZnWO_4 microspheres under UV light irradiation; photodegradation efficiencies of RhB (b) and MB (d) by different morphological ZnWO_4 as photocatalysts.

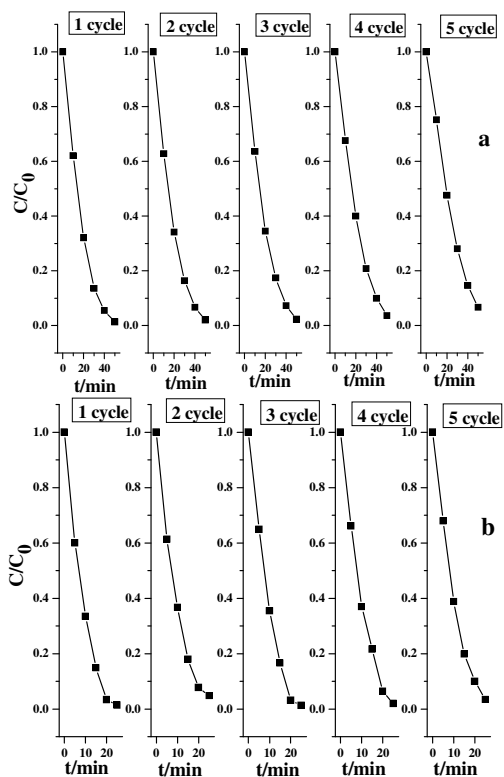


Fig. 9 Photocatalytic degradation of RhB (a) and MB (b) after five recycling runs in the presence of the yolk-shell ZnWO_4 microspheres under UV light irradiation.

Recycling and maintaining a high photocatalytic activity are critical issues for the long-term use of catalysts in practical applications. To test the stability of yolk-shell ZnWO_4 microspheres, we examined for photodegradation of RhB during cycle tests under identical conditions. Fig. 9a-b show the cycle tests of yolk-shell ZnWO_4 microspheres under UV light irradiation by the decomposition of Rhodamine B (RhB) and methylene blue (MB), respectively. After five cycles, the photocatalytic activities of the samples remained are almost unaffected, indicating that the yolk-shell ZnWO_4 microspheres are excellent catalyst during the photocatalytic decomposition of the pollutant.

25 Conclusions

A facile L-Asp assisted hydrothermal method was developed for the synthesis of yolk-shell ZnWO_4 microspheres. The amount of L-Asp, reaction time and hydrothermal temperature play key roles in the formation of different morphological ZnWO_4 micro/nanostructures. The yolk-shell ZnWO_4 microspheres present excellent photocatalytic degradation of RhB and MB under UV light irradiation. Compared with MB, RhB solution is more difficult to be decolorized. The yolk-shell ZnWO_4 microspheres can be reused up to five times, which will endow them wide applications in catalysis fields.

Acknowledgments

This work was supported by the National Natural Science Foundation of China (No. 21173122, 21376124) and Natural Science Foundation of Jiangsu Province of China (No. BK2010281).

Notes

College of Chemistry and Chemical Engineering, Nantong University, Nantong 226019, P. R. China. E-mail: hi_wangmiao@163.com; Fax: ++86-513 85012851

25 References

- Z. G. Teng, S. J. Wang, X. D. Su, G. T. Chen, Y. Liu, Z. M. Luo, W. Luo, Y. X. Tang, H. X. Ju, D. Y. Zhao and G. M. Lu, *Adv. Mater.* 2014, **26**, 3741.
- X. L. Fang, Z. H. Liu, M. F. Hsieh, M. Chen, P. X. Liu, C. Chen and N. F. Zheng, *ACS Nano*, 2012, **6**, 4434.
- J. Liu, S. Z. Qiao, S. B. Hartono and G. Q. Lu, *Angew. Chem. Int. Ed.*, 2010, **49**, 4981.
- J. C. Park and H. Song, *Nano Res.*, 2011, **4**, 33.
- X. Y. Lai, J. Li, B. A. Korge, Z. H. Dong, Z. M. Li, F. B. Su, J. Du and D. Wang, *Angew. Chem. Int. Ed.*, 2011, **50**, 2738.
- N. Liu, H. Wu, M. T. McDowell, Y. Yao, C. M. Wang and Y. Cui, *Nano Lett.*, 2012, **12**, 3315.
- H. F. Jiu, Y. X. Sun, L. X. Zhang, C. Y. Zhang, J. Zhang and J. W. Liu, *Ceram. Int.*, 2014, **40**, 3149.
- Z. M. Cui, Z. Chen, C. Y. Cao, L. Jiang and W. G. Song, *Chem. Commun.*, 2013, **49**, 2332.
- Y. Wang, F. Wang, B. Chen, H. Xu and D. Shi, *Chem. Commun.*, 2011, **47**, 10350.
- T. Yang, J. Liu, Y. Zheng, M. J. Monteiro and S. Z. Qiao, *Chem. Eur. J.*, 2013, **19**, 6942.
- Y. Liu, C. Yu, W. Dai, X. Gao, H. Qian, Y. Hu and X. Hu, *J. Alloys Compd.*, 2013, **551**, 440.
- X. J. Wu and D. Xu, *J. Am. Chem. Soc.*, 2009, **131**, 2774.
- J. H. Gao, G. L. Liang, B. Zhang, Y. Kuang, X. X. Zhang and B. Xu, *J. Am. Chem. Soc.*, 2007, **129**, 1428.
- Y. Yin, R. M. Rioux, C. K. Erdonmez, S. Hughes, G. A. Somorjai and A. P. Alivisatos, *Science*, 2004, **304**, 711.
- X. Z. Gong, Y. Yang and S. M. Huang, *J. Phys. Chem. C*, 2010, **114**, 18073.
- E. C. Cho, P. H. C. Camargo and Y. N. Xia, *Adv. Mater.*, 2010, **22**, 744.
- L. Kuai, S. Z. Wang and B. Y. Geng, *Chem. Commun.*, 2011, **47**, 6093.
- J. Li and H. C. Zeng, *J. Am. Chem. Soc.*, 2007, **129**, 15839.
- B. Liu and H. C. Zeng, *Small*, 2005, **1**, 566.
- S. J. Chen, J. H. Zhou, X. T. Chen, J. Li, L. H. Li, J. M. Hong, Z. L. Xue and X. Z. You, *Chem. Phys. Lett.*, 2003, **375**, 185.
- L. You, Y. Cao, Y. F. Sun, P. Sun, T. Zhang, Y. Du and G. Y. Lu, *Sens. Actuators B*, 2012, **161**, 799.
- S. Lin, J. B. Chen, X. L. Weng, L. Y. Yang and X. Q. Chen, *Mater. Res. Bull.*, 2009, **44**, 1102.

- 23 H. B. Fu, J. Lin, L. W. Zhang, Y. F. Zhu, *Appl. Catal., A: General*, 2006, **306**, 58.
- 24 V. V. Atuchin, E. N. Galashov, O. Y. Khyzhun, A. S. Kozhukhov, L. D. Pokrovsky and V. N. Shlegel, *Cryst. Growth Des.*, 2011, **11**, 2479.
- 25 G. B. Kumar, K. Sivaiah and S. Buddhudu, *Ceram. Int.*, 2010, **36**, 199.
- 26 G. L. Huang, C. Zhang and Y. F. Zhu, *J. Alloys Comd.*, 2007, **432**, 269.
- 27 X. Zhao and Y. F. Zhu, *Environ. Sci. Technol.*, 2006, **40**, 3367.
- 28 J. Lin, J. Lin and Y. F. Zhu, *Inorg. Chem.*, 2007, **46**, 8372.
- 29 X. Zhao, W. Q. Yao and Y. Wu, *J. Solid State Chem.*, 2006, **179**, 2562.
- 30 D. Li, R. Shi, C. S. Pan, Y. F. Zhu and H. J. Zhao, *CrystEngComm*, 2011, **13**, 4695.
- 31 T. Montini, V. Gombac, A. Hameed, L. Felisari, G. Adami and P. Fornasiero, *Chem. Phys. Lett.* 2010, **498**, 113.
- 32 B. Liu, S. H. Yu, L. J. Li, F. Zhang, Q. Zhang, M. Yoshimura and P. K. Shen, *J. Phys. Chem. B*, 2004, **108**, 2788.
- 33 K. M. Garadkar, L. A. Ghule, K. B. Sapnar and S. D. Dhole, *Mater. Res. Bull.*, 2013, **48**, 1105.
- 34 H. Lin, G. Q. Tan, W. Zhang, Y. Q. Zheng, A. Xia and H. J. Ren, *J. Clust. Sci.*, 2013, **24**, 315.
- 35 W. Zhao, X. Y. Song, G. Z. Chen and S. X. Sun, *J. Mater. Sci.*, 2009, **44**, 3082.
- 36 J. H. Huang and L. Gao, *J. Am. Ceram. Soc.*, 2006, **89**, 3877.
- 37 L. Yang, W. S. Guan, Y. S. Yan, B. Bai, K. J. Guo, F. Chen and J. Dong, *Integrated Ferroelectrics*, 2011, 127, 48.
- 38 H. X. Li, Z. F. Bian, J. Zhu, D. Q. Zhang, G. S. Li, Y. N. Huo, H. Li and Y. F. Lu, *J. Am. Chem. Soc.*, 2007, **129**, 8406.
- 39 M. Wang, Y. J. Shi, Y. F. Tang and G. Q. Jiang, *Mater. Lett.*, 2014, **122**, 66.
- 40 M. Wang, Y. J. Shi, Y. F. Tang and G. Q. Jiang, *Mater. Lett.*, 2014, **132**, 236.
- 41 Z. G. An, S. L. Pan, J. J. Zhang and G. Z. Song, *Dalton Trans.*, 2008, 5155.
- 42 G. H. Tian, Y. J. Chen, W. Zhou, K. Pan, Y. Z. Dong, C. G. Tian and H. G. Fu, *J. Mater. Chem.*, 2011, **21**, 887.
- 43 H. G. Yang and H. C. Zeng, *J. Phys. Chem. B*, 2004, **108**, 3492.
- 44 Y. Wang, Q. S. Zhu and L. Tao, *CrystEngComm*, 2011, **13**, 4652.
- 45 J. G. Yu, J. C. Yu, W. K. Ho, M. K.-P. Leung, B. Chen, G. K. Zhang and X. J. Zhao, *Appl. Catal. A*, 2003, **255**, 309.
- 46 J. C. Groen, L. A. A. Peffer and J. Perez-Ramirez, *Microporous Mesoporous Mater.*, 2003, **60**, 1
- 47 H. X. Li, Z. F. Bian, J. Zhu, D. Q. Zhang, G. S. Li, Y. N. Huo, H. Li, and Y. F. Lu, *J. Am. Chem. Soc.*, 2007, **129**, 8406.
- 48 J. W. Shi, H. J. Cui, X. Zong, S. H. Chen, J. S. Chen, B. Xu, W. Y. Yang, L. Z. Wang and M. L. Fu, *Appl. Catal. A: General*, 2012, **435**, 86.

50